We_P01_01

Pre-Processing a Land Walkaway VSP Dataset for Elastic FWI: Effects of Deconvolution Operations

R. Cova[1]*, K. Innanen[1], M. Rauch-Davies[2]

[1] University of Calgary/CREWES; [2] Devon Energy

Summary

A land VSP dataset acquired in a walkaway configuration was pre-processed for FWI purposes. Two different deconvolution approaches were studied. First, a deterministic deconvolution was applied to remove source-related effects. Even though this process partially accounts for changes in the wavelet with depth, a single operator is used for all the events recorded on a given trace. For this reason, we also applied a Gabor deconvolution to more completely account for non-stationarity in the source signature. The elastic FWI performed on the data deconvolved with deterministic operators converged toward a solution that was closer to the well log data. The FWI results using the data without deconvolution and the Gabor-deconvolved data did not converge toward a reasonable solution. A closer examination revealed that the deterministic deconvolution attenuated most of the multiples energy present in the data. This resulted in a dataset that is easier to explain by an initial smooth velocity model. Also, the deterministic deconvolution resurfaced some downgoing S-wave events that were not evident before. Providing data with less complexity and enhancing critical events resulted in a more robust initialization of the inversion problem.

Introduction

Full waveform inversion (FWI) is an iterative process for computing subsurface parameters given a set of seismic waveformrs. Its application using marine data is very well documented and many successful case studies have been reported in the literature (Ratcliffe et al., 2011; Operto et al., 2015; Routh et al., 2017). However, on land data, its application is significantly more difficult. The reasons include, but are not limited to, very complex near-surface effects, unknown source and receiver signature, strong anelasticity and poor signal-to-noise ratio particularly for the frequencies in the low end of the spectrum. These low frequencies are usually never recorded and have to be estimated.

Some of these challenges are less problematic in the case of vertical seismic profiles (VSP). Since in this type of acquisiton, receivers are placed in a borehole and only the source remains at the surface, near-surface effects tend to be limited. For the same reason, receivers are less afected by surface-related noise resulting in larger signal-to-noise ratios. Podgornova et al. (2014) and Pan et al. (2018) report successful results in performing elastic FWI over land VSP datasets. Here, we study how the pre-processing of the data affects the FWI output. Particularly, we investigate how the application or not of deconvolution opeartors affects the FWI results. The dataset we use presents very large and frequent velocity contrasts that result in very energetic short-wavelength multiples, that challenge the initialization of the inversion.

Deconvolution Tests

Two deconvolution algorithms were tested on the data. First, we tried a conventional deterministic deconvolution. In this case, the inverse of the frequency spectrum of the downgoing wavefield is used to construct the deconvolution operator. A window of 600 ms around the first arrivals was used for the computation of the spectra and a pre-whitening factor of 1% was added to stabilize the inversion of the deconvolution operators.

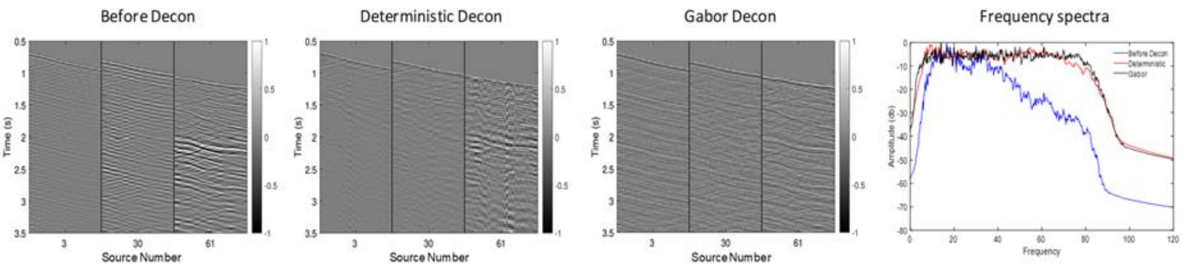

Figure 1 *Data before and after deterministic and Gabor deconvolutions and their frequency spectra.*

Figure 1 displays a subset of the vertical component data, before and after deconvolution. There we can see how the character of the events has been sharpened and the frequency spectra have been equalized. On the low end of the spectrum, the frequency band between 4 Hz and 10 Hz, now displays gains of about 20 db.

The second deconvolution approach consisted in performing a Gabor deconvolution (Margrave and Lamoureux, 2001). The goal here was to remove time-dependent source wavelet variations in a more complete fashion. This deconvolution was performed using windows of 0.2 s in increments of 0.01 s and temporal and frequency smoothers of 0.4 s and 4 Hz, respectively.

The vertical component after Gabor deconvolution are also shown in Figure 1. Similar to the deterministic deconvolution, the Gabor-deconvolved data resulted in in a wider and more equalized frequency spectrum. Moreover, the events after Gabor deconvolution display better coherency. The flat character of the frequency spectrum between 4 Hz and 80 Hz is very clear in Figure 1. Gains on the low end of the frequency spectrum are comparable with the ones obtained with the deterministic deconvolution.

Despite producing similar spectral responses, the output data present some differences. From Figure 1 it is clear that the deterministic deconvolution has collapsed many of the reverberations (multiples) present in the data into fewer events (primaries). However, for the data deconvolved with Gabor operators most of these reverberations are still present but the data seems to be better equalized. The performance of the FWI on each dataset is investigated in the next section.

Full Waveform Inversion

We used a time domain elastic FWI algorithm based on spectral elements modelling (Komatitsch and Tromp, 1999). We defined a mesh with an element size of 25 m and 5 Gauss-Lobatto-Legendre (GLL) points per element. The modelling time step was set at 3.25x10-4 s to satisfy the CFL stability condition. The initial velocity and density models were computed by smoothing the available well log data using a Gaussian smoother with a half-length of 100 m.

The inversion was carried out in three depth windows: 250 - 1000 m, 750 - 2250 m and 2000 - 3500 m. At each window the inversion was performed using a multi-scale approach using four frequency bands. We started with the band between 4-8 Hz with increments of 4 Hz on the high end of the filter up to a maximum of 24 Hz. Eight source locations were used in the inversion ranging between 113 m and 1812.5 m offset from the well.

The near-offset data for the first scale and first depth window are shown in Figure 2. The effects of the pre-processing are very clear in this example. On the data deconvolved with the deterministic operators it is possible to identify a downgoing S-wave arrival that was not evident in the data before deconvolution and is not observable in the Gabor-deconvolved data. The deterministic deconvolution, by trying to remove the effect of the downgoing wavelet, collapsed most of the downgoing P-wave energy around the direct arrivals revealing the downgoing S-wave energy present in the data.

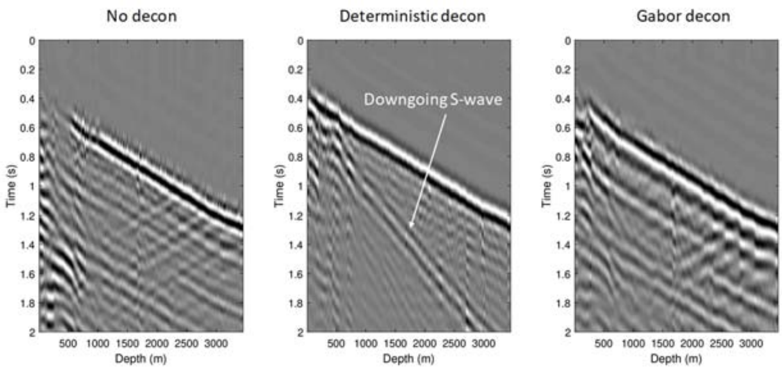

Figure 2 *Data filtered between [4-8 Hz].*

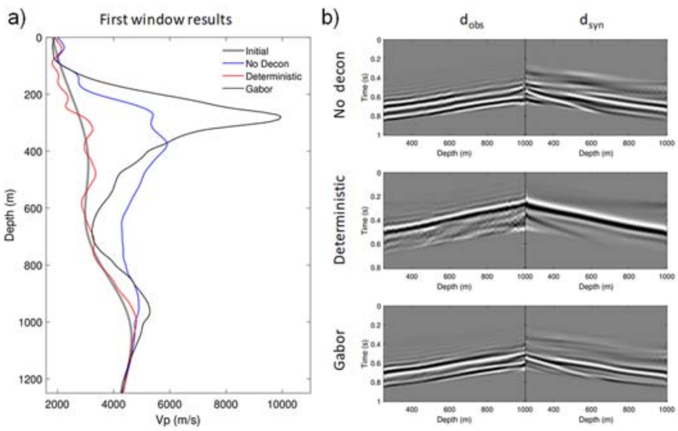

Figure 3 *(a) Inverted Vp models using the downgoing wavefields. (b) Downgoing observed and modelled data after FWI.*

To test the performance of the inversion, we first inverted the downgoing wavefield of the near-offset source with both types of deconvolution. An FK filter was applied on-the-fly to separate the downgoing wavefield from the upgoing wavefield. Only the data within a 500 ms window centered around the first arrivals were used for the inversion, the rest were muted. The inverted Vp values for this test using the first depth window are shown in Figure 3a. There, we can observe that the inversion performed with the Gabor deconvolved data is diverging significantly from the initial Vp model. Using data without any deconvolution also resulted in a divergent solution. Only the data deconvolved with deterministic operators show a stable solution, providing reasonable model updates around the initial Vp model. Figure 3b confirms these observations on the data space. There, only the data modelled after the inversion with the deterministic deconvolution closely resembles the observed data.

The previous results can be explained by the presence of long and short period interbed multiples in the data. In particular, the presence of fine layering with large velocity contrasts that results in very short-period internal multiples, introduces a coda in the downgoing wavefield that is very difficult to explain with an initial smooth velocity model.

Based on the previous results we chose to proceed with the inversion using only the data with deterministic deconvolution. We inverted for Vp and Vs, keeping the density model fixed. Figure 4 shows the results at the well location. Overall, the inverted Vp values follow very closely the expected values according to the well log data. However, the inversion underestimated the actual Vp values in the section around 1500 m depth. The results for Vs also show a good agreement in the shallow part of the section. However, for depths under 2000 m the results are mixed. We would expect these results to improve by including farther source locations with more energetic S-wave arrivals in the inversion.

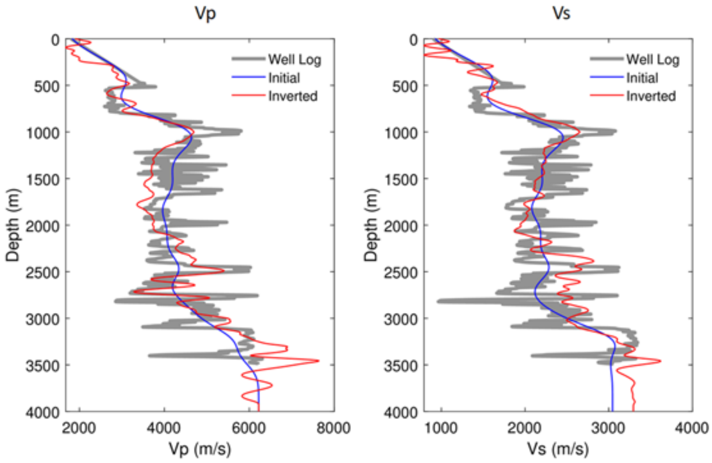

Figure 4. FWI results at the well location.

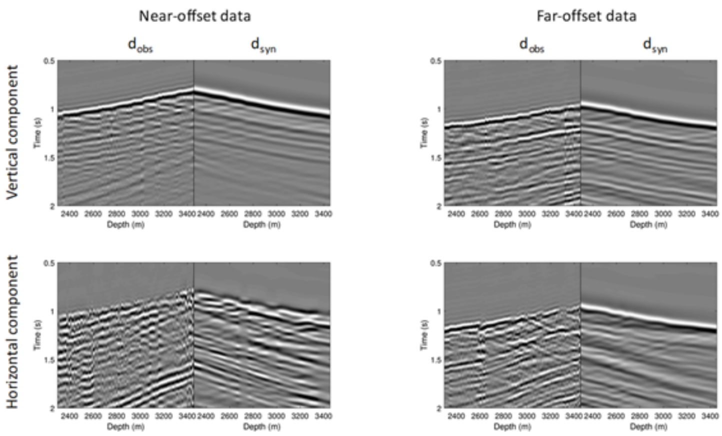

Figure 5. Observed and modelled data at the near and far offset locations, after FWI.

Figure 5 compares the observed data and the data modelled after the inversion for a near- and far-offset locations. There, we can observe a good agreement between the modelled and observed downgoing wavefields, particularly for the vertical component data at both offsets. Even some of the downgoing multiples that were attenuated in the input data, have been reproduced. On the horizontal components the results are mixed. For the near-offset data there is very little coherent energy above 1.5 s. There is a large-amplitude S-wave event around 1.75 s that is partially matched on the synthetic data. We can also observe that their frequency content is slightly different. On the far-offset data S-wave energy displays better coherency. There, we can observe a better agreement among the downgoing events on both datasets.

Conclusions

The non-linearity of the FWI problem can lead to very different solutions even when the input data are slightly different. We inverted one dataset pre-processed with two different deconvolution methods that were trying to account for the missing physics in our FWI algorithm. The data pre-processed with a deterministic deconvolution provided superior results than the ones obtained with a Gabor deconvolution. The solution obtained using data without deconvolution also diverged from the initial model. We argue that by collapsing and attenuating some of the multiples present in the data, the deterministic deconvolution provided an easier-to-model dataset given a smooth initial velocity model. By attenuating the multiples this deconvolution was also able to reveal downgoing S-wave events that were not evident before. The Gabor deconvolution provided a wider and more stable amplitude spectrum. However, the energy resulting from multiple events was left untouched, resulting in a more complex dataset. In this case, a more complex initial subsurface model might be needed for the inversion to converge toward a reasonable model.

Acknowledgements

The authors thank the sponsors of CREWES in particular to Devon Energy for facilitating the data used in this study. This work was funded by CREWES industrial sponsors, CFREF (Canada First Research Excellence Fund) and NSERC (Natural Science and Engineering Research Council of Canada) through the grant CRDPJ 461179-13. We are also grateful to Compute Canada for providing the computational resources used in this study.

References

Komatitsch, D., and Tromp, J., 1999, Introduction to the spectral-element method for 3-D seismic wave propagation: Geophysical Journal International, 139, No. 3, 806–822.

Margrave, G., and Lamoureux, M., 2001, Gabor deconvolution: CREWES Research Report, 13, 241–276.

Operto, S., Miniussi, A., Brossier, R., Combe, L., Metivier, L., Monteiller, V., Ribodetti, A., and Virieux, J., 2015, Efficient 3-d frequency-domain mono-parameter full-waveform inversion of ocean-bottom cable data: application to valhall in the visco-acoustic vertical transverse isotropic approximation: Geophysical Journal International, 202, No. 2, 1362–1391.

Pan, W., Innanen, K. A., and Geng, Y., 2018, Elastic full-waveform inversion and parametrization analysis applied to walk-away vertical seismic profile data for unconventional (heavy oil) reservoir characterization: Geophysical Journal International, 213, No. 3, 1934–1968.

Podgornova, O., Leaney, S., Charara, M., and Lunen, E. V., 2014, Elastic full waveform inversion for land walkaway VSP data: CSEG Geoconvention 2014 Expanded abstracts.

Ratcliffe, A., Win, C., Vinje, V., Conroy, G.,Warner, M., Umpleby, A., Stekl, I., Nangoo, T., and Bertrand, A., 2011, Full waveform inversion: A north sea obc case study: SEG Technical Program Expanded Abstracts 2011, 2384–2388.

Routh, P., Neelamani, R., Lu, R., Lazaratos, S., Braaksma, H., Hughes, S., Saltzer, R., Stewart, J., Naidu, K., Averill, H., Gottumukkula, V., Homonko, P., Reilly, J., and Leslie, D., 2017, Impact of high-resolution FWI in the western black sea: Revealing overburden and reservoir complexity: The Leading Edge, 36, No. 1, 60–66.